Inorg. Chem. **2006**, *45*, 3958–3963

A Computational Study of the Nondissociative Mechanisms that Interchange Apical and Equatorial Atoms in Square Pyramidal Molecules

Henry S. Rzepa*,† and Marion E. Cass‡

Department of Chemistry, Imperial College London, London SW7 2AZ, U.K., and Department of Chemistry, Carleton College, Northfield, Minnesota 55057

Received November 18, 2005

Ⓦ This paper contains enhanced objects available on the Internet at http://pubs.acs.org/journals/inocaj.

The lowest energy transition state for the nondissociative apical/equatorial atom exchange mechanism for three square pyramidal AEX_5 molecular species was calculated (CCSD(T)/pVTZ; B3LYP/pVTZ, aug-cc-pV5Z) to have a hemidirected geometry with C_s symmetry for BrF_5, IF_5, and XeF_5^+. In contrast, holodirected C_{2v}-symmetric transition states for this process were located for the AEX_5 square pyramidal molecules ClF_5, ICl_5, and IBr_5. Imaginary frequencies were calculated and examined in a visual/dynamic fashion to gain insight into these fluxional processes. Although both mechanisms exchange one apical for one equatorial atom in each cycle of motion, processes that pass through C_{2v} transition states have characteristic features of the well-known Berry pseudorotation and Lever mechanisms while those which pass through transition states of C_s symmetry have features that are a mixture of Berry, Lever, and turnstile-like character. Two periodic trends are observed: as the atomic number on the central atom increases (same terminal atoms), the barrier for apical/equatorial exchange and the value of the imaginary frequency both decrease. Similarly, as the atomic number of the terminal atoms increase (same central atom), the barrier for apical/equatorial exchange decreases, as does the computed imaginary frequency.

Introduction

Motions that exchange symmetry nonequivalent atoms within a molecule, referred to as fluxional processes or nondissociative exchange mechanisms, are documented for many chemical species. Two very well-known examples are the axial/equatorial hydrogen exchange in cyclohexane,[1] and the Berry pseudorotation (BPR) that exchanges the axial and equatorial atoms in trigonal bipyramidal molecules such as PF_5.[2] Similar mechanisms, that interchange symmetry nonequivalent terminal atoms in a nondissociative fashion, have been reported in the literature for several other small molecules: These include the Lever mechanism (observed for ClF_3 and in one high-energy pathway for SF_4),[3,4] the BPR for disphenoidal molecules, (observed for SF_4, for $X(CH_3)_4$ where X = S, Se, and Te, and in $X(R'N{-}CR{-}NR')_2$ where X = Si, Ge, Sn, and Pb),[4−6] the turnstile mechanism (experimentally observed in the fluxional processes of several Mo(II) complexes[7] and calculated for the cis/trans isomerization for SF_4Cl_2 [8]) and the Bartell Mechanism observed for apical/equatorial atom exchange in IF_7.[9] Animations of

* To whom correspondence should be addressed.
† Imperial College London.
‡ Carleton College.

(1) Carey, F. A. *Organic Chemistry*, 4th ed.; McGraw-Hill: New York, 2000; p 511. Komornicki, A.; McIver, J. W., Jr. *J. Am. Chem. Soc.* **1973**, *95*, 4512−4517.
(2) Berry, R. S. *J. Chem. Phys.* **1960**, *32*, 933−938. Bartell, L. S.; Kutchitsu, K.; eNeui R. J. *J. Chem. Phys.* **1961**, *35*, 1961, 1211.
(3) Cleveland, T.; Landis, C. R. *J. Am. Chem. Soc.* **1996**, *118*, 6020−6030.
(4) Mauksch, M.; Schleyer, P. von R. *Inorg. Chem.* **2001**, *40*, 1756−1769.
(5) Marsden, C. J.; Smart, B. A. *Organometallics* **1995**, 5399−5409. Fowler, J. E.; Schaefer, H. F. *J. Am. Chem. Soc.* **1994**, *116*, 9596−9601.
(6) Kilimann, U.; Noltemeyer, M.; Edelmann, F. T. *J. Organomet. Chem.* **1993**, *443*, 35−42. Karsch, H. H.; Scluter, P. A.; Reisky; M. *Eur. J. Inorg. Chem.* **1998**, 433−436. Schoeller, W. W.; Sundermann, A.; Reiher, M. *Inorg. Chem.* **1999**, *38*, 29−37.
(7) Shiu, K. B.; Liou, K. S.; Cheng, C. P.; Rang, B. R.; Wang, Y.; Lee, G. H.; Vong, W. J. *Organometallics* **1989**, *8*, 1219−1224. Espinet, P.; Hernando, R.; Itrube, G.; Villafane, F.; Orpen, A. G.; Pascual, I. *Eur. J. Inorg. Chem.* **1998**, 433−436.
(8) Cass, M. E.; Hii, K. K.; Rzepa, H. S. *J. Chem. Educ.* **2006**, *83*, 336.
(9) Adams, W. J.; Thompson, H. B.; Bartell, L. S. *J. Chem. Phys.* **1970**, *53*, 4040−4046. Bartell, L. S.; Rothman, M. J.; Gavezzotti, A. *ibid* **1982**, *76*, 4136−4413. Christe, K. O.; Curtis, E. C.; Dixon, D. A. *J. Am. Chem. Soc.* **1993**, *115*, 1520−1526.

10.1021/ic0519988 CCC: $33.50
Published on Web 04/20/2006

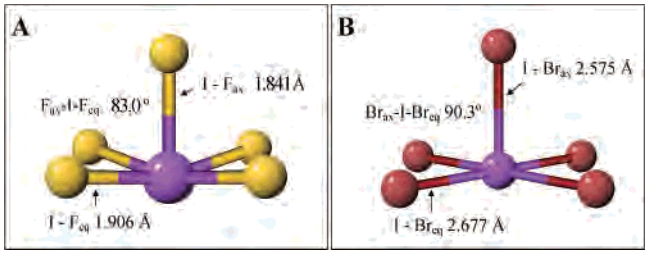

Figure 1. Equilibrium geometries for (A) IF_5 (B3LYP/aug-cc-pV5Z-pp) and (B) IBr_5 (B3LYP/pVTZ).

Ⓦ Animations of the apical/equatorial atom exchange mechanisms for ClF_5, BrF_5, IF_5, ICl_5, IBr_5, and XeF_5^+ are available, together with animations for the pure BPR mechanism of apical/equatorial atom exchange for PF_5, the pure Lever mechanism of apical/equatorial atom exchange for ClF_3 and the pure turnstile mechanism of apical/equatorial atom exchange for SF_4Cl_2. Equilibrium geometries (giving bond lengths and bond angles) and transition state structures are included.

the BPR in PF_5, the Lever Mechanism in ClF_3, and the turnstile mechanism can be found in ref 8 and/or in our supplemental material [enhanced Web objects 9a, 9b, and 9c, respectively] for comparison to the mechanisms described herein.

Surprisingly, very little quantitative information is available on the apical/equatorial atom exchange in square pyramidal AEX_5 molecules (using VSEPR nomenclature where A represents the central atom, E an electron lone pair, and X the terminal atoms). Representative square pyramidal ground-state structures of IF_5 and IBr_5 are shown in Figure 1. Early variable-temperature ^{19}F NMR studies on IF_5, BrF_5, and ClF_5 showed[10,11] that these three species were stable to apical/equatorial exchange at room temperature, implying barriers for the process of greater than approximately 25 kcal mol^{-1}. No terminal atom exchange was observed for BrF_5 at elevated temperatures; however, under the same conditions, IF_5 began to lose F−F coupling and then broaden, characteristic of apical/equatorial atom exchange.[10] Although the exchange was proposed to proceed through an associative/dissociative process (via either bridging fluorines in dimers or by heterolytic dissociation), this early research established that the barrier for any fluxional process in these square pyramidal molecules, regardless of whether they are associative/dissociative or nondissociative, must be significantly larger than the barriers observed for similar small molecules such as PF_5 and IF_7 which are known to be highly fluxional.

We report herein our computational study of the nondissociative mechanisms that interchange apical and equatorial atoms in the square pyramidal AEX_5 molecular species ClF_5, BrF_5, IF_5, ICl_5, IBr_5, and XeF_5^+. We have found that these nondissociative exchange mechanisms proceed through one of two pathways; one that proceeds through a C_s transition state (for BrF_5, IF_5, and XeF_5^+) which we describe as "hemidirected", or through a C_{2v} transition state (for ClF_5, ICl_5, and IBr_5) which we describe as "holodirected". We have

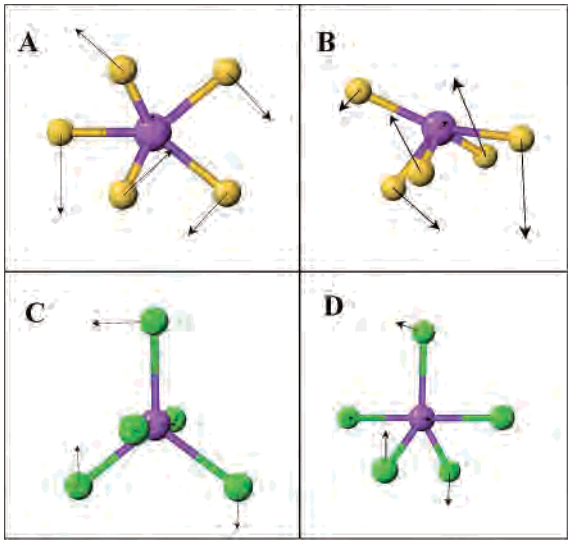

Figure 2. (A and B) Two orientations of the hemidirected C_s transition state for BrF_5 shown with the displacement vectors of the calculated imaginary frequency. View B illustrates "the void" of coordinated atoms in the top hemisphere of the structure. (C and D) Two orientations of the holodirected C_{2v} transition-state structure for ICl_5 also showing the displacement vectors for the calculated single imaginary frequency. Note that the mode of the imaginary frequency primarily involves the four coplanar (three equatorial Cl's and the central I) atoms.

borrowed the holodirected and hemidirected descriptors from the literature, where they are used to denote the distribution of ligands around the central metal ion in complexes of, e.g., lead or tin. A holodirected geometry is one "in which the bonds to ligands atoms are distributed throughout the surface of an encompassing globe".[12] In contrast a hemidirected geometry is one "in which the bonds to ligand atoms are directed throughout only part of an encompassing globe, i.e., there is an identifiable void in the distribution of bonds to the ligands."[12] Application of these descriptors to our two transition-state geometries seems wholely appropriate, as the C_s transition state clearly has "a void" on one side (see Figure 2B), and in the C_{2v} transition state, the terminal atoms are "distributed throughout" the surface of an encompassing globe (Figure 2C and D).

In addition to examining the geometry and symmetry of the transition states in these reactions, we have also examined the motion of the apical/equatorial exchange mechanisms by animating the calculated imaginary frequency of the transition state. Following either the positive or the negative displacement of the imaginary frequency along the potential surface lowers the energy and eventually would lead to either the reactant or the product of the reaction. We can therefore use the output vibrational information from our computation to visually examine the operative exchange mechanism for a molecule under question. We observe distinctly different types of motion based on whether the mechanism proceeds through a hemidirected C_s transition state or a holodirected C_{2v} transition state. Visual/dynamic analysis was crucial to our understanding of these mechanisms and we therefore strongly encourage the reader to go to our supplemental

(10) Muetterties, E. L.; Phillips, W. D. *J. Am. Chem. Soc.* **1957**, *79*, 322−326.
(11) Bantov, D. V.; Dzevitskii, B. E.; Konstantinov, Y. S.; Sukhoverkhov, V. F. *Izv. Sib. Otd. Akad. Nauk SSSR, Ser. Khim. Nauk.* **1968**, *1*, 81−3.
(12) Shimoni-Livny, L.; Glusker, J. P.; Bock, C. W. *Inorg. Chem.* **1998**, *37*, 1853−1867.

Table 1. Calculated Energies for Nondissociative Fluxional Apical/Equatorial Atom Exchange in Square Pyramidal AEX_5 Molecules

AEX_5	calculation method/ basis set	ground-state energy in Hartrees	symmetry	barrier kcal/mol	imaginary frequency in cm^{-1}	WEO ref	notes
ClF_5	CCSD(T)/pVTZ	−957.62901	C_s	40.5	–		[a]
			C_{2v}	33.4	–		[b]
	B3LYP/aug-cc-pV5Z	−959.35502	C_s	40.2	199.4	Suppl. 3b	[c]
			C_{2v}	36.5	328.5	Suppl. 3a	
	B3LYP/pVTZ	−959.21305	–		–		[d]
			C_{2v}	29.1	267		[e,f]
	KMLYP/pVTZ	−957.84872	C_s	53.2	251.1		
			C_{2v}	57.3	454.1		
BrF_5	CCSD(T)/pVTZ	−3071.01275	C_s	35.6	–		[a]
			C_{2v}	36.8	–		[b]
	B3LYP/aug-cc-pV5Z	−3073.45244	C_s	31.9	171.3		[g]
			C_{2v}	31.9	254.2	Suppl. 4b	[g]
	B3LYP/pVTZ	−3073.26470	C_s	31.9	171.2	Suppl. 4a	[h]
			C_{2v}	29.3	240.6		
	KMLYP/pVTZ	−3071.26094	C_s	43.9	214.1		[h,f]
			C_{2v}	54.3	371.7		
IF_5	CCSD(T)/pVTZ	−7416.65020	C_s	29.3	–		[a]
			C_{2v}	49.5	–		[b]
	B3LYP/aug-cc-pV5Z-pp	−797.17427	C_s	24.7	139.8	Suppl. 5a	[i]
	B3LYP/pVTZ	−7419.82665	C_s	26.7	150.6		[j]
			D_{3h}	44.8	180.3	Suppl. 5b	[k]
			C_{2v}	40.9	258.0	Suppl. 5c	[l]
	KMLYP/pVTZ	−7417.18400	C_s	32.3	172.5		[f]
			D_{3h}	76.7	285.7		[m]
ICl_5	B3LYP/pVTZ	−9221.58867	C_{2v}	11.5	69.3	Suppl. 6a	[e]
			D_{3h}	11.7	44.2	Suppl. 6b	[k]
	KMLYP/pVTZ	−9217.79738	C_s	29.9	93.4		[f]
			C_{2v}	28.6	157.4		[f]
IBr_5	B3LYP/pVTZ	−19791.25590	C_{2v}	4.9	25.2	Suppl. 7	[h]
	KMLYP/pVTZ	−19784.21444	C_{2v}	19.1	80.5	–	[h]
XeF_5^+	B3LYP/cc-pV5Z-pp	−828.17381	C_s	28.3	154.4	Suppl. 8	[n]

[a] CCSD(T) energy at CCSD geometry. No frequencies available. [b] 3-ζ on F, Cl, coupled cluster singles doubles. [c] Correlation consistent aug-5-ζ on F, Cl. [d] Geometry collapses to ground state. [e] 3-ζ on F, Cl. [f] KMLYP method. [g] Correlation consistent aug-5-ζ on F, Br. $\Delta G_{298^\ddagger}$ 30.5 (C_s)/28.8 (C_{2v}) kcal mol^{-1}. [h] 3-ζ on F, Br. [i] Correlation consistent aug-5-ζ on F, aug-5-ζ+ECP on I. $\Delta G_{298^\ddagger}$ 23.8 kcal mol^{-1}. [j] 3-ζ on F, I. [k] Transition mode degenerate. [l] Second imaginary mode −75.3 cm^{-1}. [m] Third imaginary mode: −110.0 reduces symmetry to C_{3v}. [n] Correlation consistent aug-5-ζ on F, aug-5-ζ+ECP on Xe.

material to view the three-dimensional animations that we have provided which include interactive content to illustrate the points we will make within this paper.

Results

Ground-State Structures. The computed ground-state structures of ClF_5, BrF_5, IF_5, ICl_5, IBr_5, and XeF_5^+ all have square pyramidal geometry with C_{4v} symmetry. Computational methods and ground-state energies are listed in Table 1. The computational methods were chosen to match those carried out to locate transition states and are therefore discussed vida infra. All species are AEX_5 VSEPR structures with one central atom (A), one electron pair (E), and five terminal atoms: one in an apical position and four others sitting in symmetry-equivalent equatorial positions. The geometry varies only slightly within the series from a nearly perfect square pyramid in IBr_5 (Figure 1B) to a somewhat distorted square pyramidal structure for IF_5 (Figure 1A) with $F_{axial}-I-F_{equatorial}$ angles of 83.0°. (See Supplement 1 for three-dimensional movable images of the equilibrium geometry computed for each molecular species in this study and for the comparison of computed bond lengths and angles to those reported in the literature for known structures).

Transition-State Structures. The fluxional processes for all of the molecules examined in this study have motions that appear to have some mixture of the physical characteristics of the BPR, turnstile, and Lever mechanisms. The molecules that have fluxional processes that pass through transition states with C_s symmetry (BrF_5, IF_5, and XeF_5^+) exhibit characteristics from all three motions; Berry, turnstile, and Lever. In recognition of this mixed character, we have christened this a "chimeric pseudorotation".[8] In contrast, ClF_5, ICl_5, and IBr_5 pass through transition states of C_{2v} symmetry and exhibit only Lever and Berry character, with dominance of the Lever character in transition states that approach D_{3h} symmetry (to see animations of the BPR, Lever, and turnstile mechanims, see Supplement 9a, 9b, and 9c, respectively, or to the animations provided in ref 8).

Transition states were located using the following protocols (see Table 1); (a) using the triple-ζ basis reported by Sadlej[13] and the B3LYP density functional hybridization. (b) We have previously reported on inter-halogen compounds[14] for which

(13) Sadlej, A. J. *Collect. Czech. Chem. Commun.* **1988**, *53*, 1995. Sadlej, A. J.; Urban, M. *J. Mol. Struct. (THEOCHEM)* **1991**, *234*, 147. Sadlej, A. J. *Theor. Chim. Acta* **1992**, *79*, 123. Sadlej, A. J. *Theor. Chim. Acta* **1992**, *81*, 45. Sadlej, A. J. *Theor. Chim. Acta* **1992**, *81*, 339.

a different hybridization of the density functional approach known as KMLYP[15] was suggested as resulting in improved treatment of the electron correlation of such systems with reference to the more complete (but computationally very much slower) coupled cluster (CCSD(T)) approach. (c) We include here several results at the CCSD level (for optimized geometries) and CCSD(T) for single-point energies for comparison. (d) To evaluate behavior toward the basis set limit, calculations at the correlation consistent 5-ζ level (aug-cc-pV5Z) level are also included.

Transition States of C_s Symmetry (Hemidirected). The nondissociative apical/equatorial atom exchange mechanisms for BrF_5, IF_5, and XeF_5^+ proceed through transition states that have C_s symmetry. Two orientations of the C_s transition state for BrF_5 are shown in Figure 2A and B.

BrF_5. Each method predicts both C_s and C_{2v} symmetric transition states to coexist on the potential surface and to be relatively similar in energy. B3LYP/cc-pV5Z and B3LYP/pVTZ indicate the C_{2v} transition state to be lower in energy than that of the C_s transition state, although for the former, it is only by 0.1 kcal/mol. The CCSD(T) and KMLYP calculations both found the C_s geometry as having the lowest energy, and we assign the fluxional behavior in BrF_5 to proceed through a true transition state of C_s symmetry. Animation of the single computed imaginary frequency can be viewed in Supplement 4a. Animation of the imaginary frequency calculated for the C_{2v} stationary point of higher energy can be found in Supplement 4b for comparison.

IF_5. Only a transition state of C_s geometry with a single imaginary frequency could be located for IF_5 at any of the computational methods. The form of this mode when animated (Supplement 5a) shows what we term chimeric behavior. Stationary points with D_{3h} symmetry and C_{2v} symmetry were also located; the former stationary point has a degenerate (E) imaginary mode; animation of each mode (Supplement 5b) illustrates that one has a combined Lever and Berry character, while the other mixes Berry character with a stretching motion. The stationary point of lower C_{2v} also yields two imaginary frequencies, but these are no longer degenerate. The larger of these shows both Lever and Berry character and the smaller shows a "wag" nature that does not result in the exchange of apical and equatorial atoms but if followed reduces the symmetry further to C_s (see Supplement 5c for visualization of these imaginary frequencies).

XeF_5^+. A transition state of C_s symmetry with a single imaginary frequency was the only one that could be located. Examination of the animation of the imaginary frequency (Supplement 8) confirms that the mode is chimeric in nature.

Transition States of C_{2v} Symmetry (Holodirected). The nondissociative apical/equatorial atom exchange mechanisms for ClF_5, ICl_5, and IBr_5 proceed through transition states that have C_{2v} rather than C_s symmetry. Two orientations of the C_{2v} transition state for ICl_5 are shown in Figure 2C and D. Other symmetries (C_s and D_{3h}) were also explored.

ClF_5. Although a transition state of C_s symmetry can be located using the KLMYP hybrid, which is lower in energy than that found for C_{2v} symmetry, the CCSD(T) and B3LYP calculations both invert this energy ordering, predicting C_{2v} to be the true transition state with the appropriate single imaginary frequency and displacement coordinates. On the basis that the CCSD(T) method is likely to give the most reliable result, we conclude that the apical/equatorial exchange mechanism for ClF_5 proceeds through a C_{2v}-symmetric transition state. Examination of the animated imaginary frequency for this transition state (Supplement 3a) allows one to recognize the Berry-like and Lever-like character. Unlike the apical/exchange mechanisms that proceed through a C_s transition state, no twisting (turnstile) motion is observed. The four atoms contained within the plane involved in the Lever motion show no out-of-plane deformation, as is illustrated (in the analogous ICl_5 case) by the vectors in Figure 2C and D, and can be observed in a visual/dynamic fashion in Supplement 3a. We have found this absence of out-of-plane deformation to be a signature of mechanisms proceeding through C_{2v} transition states in apical/equatorial exchange for the square planar AEX_5 molecules in our study. The imaginary mode calculated for the C_s stationary point was also animated and is presented in Supplement 3b for comparison.

ICl_5. B3LYP and KLMYP DFT calculations enable location of a true transition state of C_{2v} symmetry for ICl_5 with a single imaginary frequency. Only the KMLYP procedure enables a second transition state of C_s symmetry (of higher energy) to be located. This system is too large for a CCSD(T) calculation to be performed, but extrapolating from the previous CCSD(T) results suggest that KMLYP overemphasizes the stability of the C_s structure. Animation of the displacement vectors for the imaginary frequency for the C_{2v} transition state (Supplement 6a) illustrates that the mode, like that observed for ClF_5, has no out-of-plane deformation for the atoms involved in the Lever motion. Unlike in ClF_5, however, the mode is predominantly Lever in character and only exhibits a small amount of Berry-like character. The stationary point of D_{3h} symmetry for ICl_5 has also been calculated, and the degenerate imaginary frequencies have been animated (Supplement 6b). Analogous to the D_{3h} stationary point found for IF_5, this stationary point has a degenerate mode: one is of primary Lever character, and the other mode is of Berry-like character, mixed with a stretching motion.

IBr_5. B3LYP and KLMYP calculations for IBr_5 both allow only location of a transition state with C_{2v} symmetry, with a lower barrier than that observed for ICl_5. Animation of the single imaginary frequency found in the calculation (Supplement 7) illustrates that the mode has no out-of-plane deformation for the atoms involved in the Lever motion. This mode is even more dominantly Lever in character than that observed for ICl_5 and exhibits an almost undetectable degree of Berry-like character. Attempts to locate a stationary point

(14) Asseily, G. A.; Davies, R. P.; Rzepa, H. S.; White, A. J. P. *New J. Chem.* **2005**, *29*, 315−319.
(15) Kang, J. K.; Musgrave, C. B. *J. Chem. Phys.* **2001**, *115*, 11040−51. Senosiain, H. J. P.; Musgrave, C. B.; Golden, D. M. *Faraday Discuss.* **2001**, *119*, 173−89.

of C_s symmetry result in collapse of the geometry to a ground-state structure/energy.

Basis Set and Correlation Effects. In general, the triple- and the 5-ζ (aug-cc-pV5Z) basis sets are fairly congruent, the largest deviation being the predicted barrier for ClF_5 and associated imaginary mode frequency. More difference is observed between the B3LYP and KMLYP density functional hybrids; the former favoring C_{2v} symmetry, the latter C_s. Adjudication using the CCSD(T) procedure for BrF_5 suggests the most realistic estimate of the balance between the two symmetries is closer to that predicted by the B3LYP than the KMLYP method; use of the latter should probably be deprecated for such systems. The barrier heights predicted by B3LYP and CCSD(T) agree very well, and again, KMLYP appears to significantly overestimate their values. No accurately measured experimental values are available for comparison.

Discussion

Computationally, we have located a transition state that links two ground-state structures via a nondissociative apical/equatorial atom exchange process for all of the AEX_5 molecular species examined in this study. In all cases, the nondissociative process exchanges one apical atom for one equatorial atom in a single concerted motion. This one-for-one exchange can be easily visualized in our supplemental materials, where we have provided animations to view the exchange mechanisms. Although each cycle exchanges only two atoms, several cycles of motion can completely scramble the apical and equatorial atoms. In contrast, the BPR mechanism, (observed in trigonal bipyramidal molecules of which PF_5 is the quintessential example and disphenoidal (seesaw) molecules of which SF_4 is an example) and the Bartell Mechanism (observed for IF_7) concertedly exchange two apical atoms for two equatorial atoms.[2,16] Animations of the BPR and Bartell Mechanism can be found in Supplement 9 or elsewhere for comparison.[8] Again, several cycles of BPR or several cycles of exchange through a Bartell mechanism will completely scramble the apical/equatorial atoms in a molecule. Interestingly, although all of the AEX_5 molecular species proceed via exchange of one apical atom for one equatorial atom and begin from, and end in, a square pyramidal ground-state structure, two types of pathways are observed; one that passes through a transition state of C_{2v} symmetry that may be described as a holodirected structure and one that passes through a transition state of C_s symmetry that may be described as a hemidirected structure.

Why some species (IF_5, BrF_5, and XeF_5^+) pass through a C_s hemidirected transition state, and others (ClF_5, ICl_5, and IBr_5) pass through a C_{2v} holodirected transition state is not altogether clear to us, however. Interestingly, all the molecular species that "appropriate" the least amount of room for the lone pair on the central atom in the ground state (i.e., the bonding pairs and lone pair have similar space requirements) have C_{2v} holodirected transition states. In contrast, all of the molecular species that "appropriate" the most room for the lone pair on the central atom in the ground state have transition states of C_s hemidirected geometry. Thus, although all the molecular species we have examined in this study have hemidirected ground-state structures (to accommodate the lone pair of electrons on the central atom), those which are "more hemidirected" pass through hemidirected C_s transition states.

The mechanisms for apical/equatorial exchange (operative for IF_5, BrF_5, and XeF_5^+) that proceed through a C_s transition state are all "chimeric" in nature. This chimeric mode has features that can be recognized visually that are Berry-like, Lever-like, and turnstile-like motions. Interactive animations of apical/equatorial atom exchange that proceed through pure Berry (for PF_5), pure Lever (for ClF_3), and pure turnstile (for SF_4Cl_2) mechanisms have been included in the supplemental material (Supplements 9a, 9b, and 9c, respectively) for comparison. Symmetry analysis of the vibrational modes available to AEX_5 species with C_s symmetry indicates that there are seven A′ symmetric modes and five A″ asymmetric modes. All A′ modes are symmetrically allowed to mix with other A′ modes, and all A″ modes are allowed to mix with other A″ modes. It is not surprising, therefore, that the imaginary frequency of the C_s transition state (which has A″ symmetry: antisymmetric with respect to the plane of symmetry) has highly mixed character.

The mechanisms for apical/equatorial exchange that pass through C_{2v} transition states have "LeverBerry" character, character that is both Lever-like and Berry-like. We reiterate that, unlike apical/exchange that proceeds through a C_s transition state, no twisting (turnstile) motion is observed. The four atoms contained within the plane involved in the Lever motion show no out-of-plane deformation (see the vectors in Figure 2C and D and a visual/dynamic treatment in Supplements 4b, 6a, 7). This absence of out-of-plane deformation seems to be a signature of the exchange mechanisms proceeding through a C_{2v} transition state. In the ICl_5 and IBr_5 molecules with larger terminal atoms and longer bonds, the Lever character dominates in the vibrational mode of the imaginary frequency. A symmetry analysis for the vibrational modes for an AEX_5 species of C_{2v} symmetry yields 12 modes ($5A_1$, A_2, $3B_1$, and $3B_2$) and examination of the "LeverBerry" mode allows one to identify it as having B_1 symmetry. Interestingly, when C_{2v} symmetry is imposed on IF_5 (which has a C_s transition state), two imaginary frequencies are found: one of B_1 symmetry and "LeverBerry" in character and a second of B_2 symmetry. Animation of these modes for the stationary point of C_{2v} symmetry can be found in the supplemental material (Supplement 5c).

Two periodic trends can be seen within our computational data. Within a series with the same terminal atoms (ClF_5, BrF_5, and IF_5), as the atomic number on the central atom increases, the barrier for axial/equatorial exchange decreases (and the calculated energy of the imaginary frequency decreases as well). Therefore, when we compare the computed barriers for the same computational method (B3LYP/cc-pV5Z), the barrier for apical/equatorial atom exchange decreases across the series ClF_5 (36.5 kcal/mol) > BrF_5 (31.9 kcal/mol) > IF_5 (24.7 kcal/mol). This is consistent through-

(16) Whitesides, G. M.; Mitchell, H. G. *J. Am. Chem. Soc.* **1969**, *91*, 5384.

out the different computational methods: (KMLYP/pVTZ), ClF_5 (53.2 kcal/mol) > BrF_5 (43.9 kcal/mol) > IF_5 (32.3 kcal/mol); (CCSD(T)/pVTZ), ClF_5 (40.5 kcal/mol) > BrF_5 (35.6 kcal/mol) > IF_5 (29.3 kcal/mol). The same periodic trend was observed in two different computational studies examining apical/equatorial atom exchange in disphenoidal $X(CH_3)_4$ molecules where the barrier decreased across the series from S to Te, $S(CH_3)_4$ > $Se(CH_3)_4$ > $Te(CH_3)_4$, consistent with experimental observations.[5] This periodic trend was also reported in a computational study of the fluxional character in bis amidinate complexes ($X(R'N{-}CR{-}NR')_2$) of silicon, germanium, tin, and lead where the barrier for apical/equatorial atom exchange decreases across the series Si > Ge > Sn > Pb.[6]

Finally, if we compare the barriers within a series of AEX_5 molecules with the same central atom, as the atomic number of the terminal atoms increases, the barrier for apical/equatorial exchange decreases, as does the computed imaginary frequency. The barrier and imaginary frequencies decrease across the series (B3LYP/pVTZ calculation), IF_5 (26.7 kcal/mol and 151*i* cm^{-1} > ICl_5 (11.5 kcal/mol and 69.3*i* cm^{-1}) > IBr_5 (4.9 kcal/mol and 25.2*i* cm^{-1}). Within this series, the mechanism with the highest barrier proceeds through a hemidirected transition state of C_s symmetry, and those with a lower barrier proceed through a holodirected transition state of C_{2v} symmetry.

Computational Procedures

All calculations were performed using Gaussian 03.[17] Basis sets were either internal or incorporated as a general basis;[18] the only use of an effective core potential was the correlation-consistent cc-pV5Z-pp basis for iodine.[18] Symmetry was utilized throughout. Transition states were computed from an initially calculated Hessian, and resulting stationary points checked for the appropriate characteristics based on the number of computed negative roots in the Hessian matrix. Transition states at the CCSD level were located using an initial Hessian computed at the B3LYP level, and the CCSD(T) energy calculated at the resulting optimized CCSD geometry.

Animations (found in our enhanced Web objects) of the exchange mechanisms were created using the molecular 3D visualizer Jmol[19] and using Gaussview[20] or Chem 3D[21] as supporting programs to generate alternative orientations for the molecular species from Gaussian log or output files.

Conclusions

In our computational study on nondissociative mechanisms that interchange apical and equatorial atoms in square pyramidal AEX_5 molecules, we have found two pathways for terminal atom exchange: one which proceeds through a transition state of C_s symmetry and a second which proceeds through a transition state of C_{2v} symmetry. The C_s transition states located for BrF_5, IF_5, and XeF_5^+ have hemidirected geometries in which the terminal atoms are distributed in such a fashion as to create a coordination void in one hemisphere. In contrast, the C_{2v} transition states located for ClF_5, ICl_5, and IBr_5 have terminal atoms that are spatially more equally distributed about the central atom in what is referred to as a holodirected geometry. The molecular motions of the apical/equatorial exchange mechanisms also differ on the basis of whether they proceed through a transition state of C_s symmetry or a transition state of C_{2v} symmetry. Animation of the imaginary frequencies computed for the transition states allowed us to examine the mechanistic motions in a visual/dynamic fashion. In both pathways, one apical atom is exchanged for one equatorial atom in each cycle of motion. The mechanisms for apical/equatorial atom exchange in those species which pass through transition states of C_s symmetry have chimeric character with Berry-like, Lever-like, and turnstile-like features. In contrast, the mechanisms that proceed through C_{2v} transition states are also chimeric in nature but lack twisting (turnstile) character. The ground-state structures for all of the molecular species examined in this study (ClF_5, BrF_5, IF_5, ICl_5, IBr_5, and XeF_5^+) have square pyramidal geometry with C_{4v} symmetry.

The calculated barrier for apical/equatorial exchange decreases as the atomic number of the central atom increases (within a series with the same terminal atom): ClF_5 > BrF_5 > IF_5. Similarly, The calculated barrier for apical/equatorial exchange decreases as the atomic number of the terminal atoms increase (within a series with the same central atom): ClF_5 > ICl_5 > IBr_5.

Acknowledgment. M.E.C., the Charles "Jim" and Marjorie Kade Professor of the Sciences, would like to thank the Kades for their generous support of Carleton College. M.E.C. would also like to thank Henry Rzepa and the Department of Chemistry at Imperial College London for hosting her while on sabbatical leave.

IC0519988

(17) Frisch, M. J.; Trucks, G. W.; Schlegel, H. B.; Scuseria, G. E.; Robb, M. A.; Cheeseman, J. R.; Montgomery, J. A., Jr.; Vreven, T.; Kudin, K. N.; Burant, J. C.; Millam, J. M.; Iyengar, S. S.; Tomasi, J.; Barone, V.; Mennucci, B.; Cossi, M.; Scalmani, G.; Rega, N.; Petersson, G. A.; Nakatsuji, H.; Hada, M.; Ehara, M.; Toyota, K.; Fukuda, R.; Hasegawa, J.; Ishida, M.; Nakajima, T.; Honda, Y.; Kitao, O.; Nakai, H.; Klene, M.; Li, X.; Knox, J. E.; Hratchian, H. P.; Cross, J. B.; Bakken, V.; Adamo, C.; Jaramillo, J.; Gomperts, R.; Stratmann, R. E.; Yazyev, O.; Austin, A. J.; Cammi, R.; Pomelli, C.; Ochterski, J. W.; Ayala, P. Y.; Morokuma, K.; Voth, G. A.; Salvador, P.; Dannenberg, J. J.; Zakrzewski, V. G.; Dapprich, S.; Daniels, A. D.; Strain, M. C.; Farkas, O.; Malick, D. K.; Rabuck, A. D.; Raghavachari, K.; Foresman, J. B.; Ortiz, J. V.; Cui, Q.; Baboul, A. G.; Clifford, S.; Cioslowski, J.; Stefanov, B. B.; Liu, G.; Liashenko, A.; Piskorz, P.; Komaromi, I.; Martin, R. L.; Fox, D. J.; Keith, T.; Al-Laham, M. A.; Peng, C. Y.; Nanayakkara, A.; Challacombe, M.; Gill, P. M. W.; Johnson, B.; Chen, W.; Wong, M. W.; Gonzalez, C.; Pople, J. A. *Gaussian 03*, revision C.01; Gaussian, Inc.: Wallingford, CT, 2004.

(18) http://www.emsl.pnl.gov/forms/basisform.html

(19) See http://jmol.sourceforge.net/

(20) *Gaussview*, Version 3.0; Gaussian: (see reference for Gaussian).

(21) *CS Chem3D Ultra*, Version 7.0.0; CambridgeSoft: Cambridge, MA, 2001.